

Effect of Acid Concentration and Time on Synthesizing the Titanium Dioxide from Synthetic Rutile Waste

Huzaikha Binti Awang¹, Ahmad Mukifza², Shahril Yusof³, Clarence Ongkudon⁴,
Eddy Mohd Farid⁵

^{1,2,3}Faculty of Engineering

⁴Biotechnology Research Institute

⁵Faculty Science and Natural Resources

Abstract: A fast and easy method for preparing the titanium dioxide (TiO₂), using a caustic hydrothermal decomposition conditions followed with sulphate process using sulfuric acid (H₂SO₄) are presented. The effects of acid concentration and treatment time of sulphate process to the TiO₂ growth were focused in this research. The chemical composition of the product will be characterized using Electron Dispersive (EDX), the morphology and growth of titanium were analysed using a Field Emission Scanning Electron Microscope (FESEM) and the crystallinity of sample were analysed by X-Ray Diffraction (XRD). From this research work, we found that the caustic hydrothermal decomposition method followed with sulphate process has been proven to extract a titanium nanocrystals with the average mean size < 100nm after treated with medium acid concentration and short treatment time.

Keywords: Synthetic rutile; titanium dioxide; caustic hydrothermal decomposition; Sodium titanate; sulphate process.

I. INTRODUCTION

The production of TiO₂ has been applied commercially since 1923 [1]. The main mineral use to produce a TiO₂ are ilmenite, rutile raw materials and leucosene [2]. The main minerals to synthesis the TiO₂ are Ilmenite, leucosene and rutile. The ilmenite, leucosene and rutile contains about 40–65%, more than 65% and 95% TiO₂ respectively [3]. The Synthetic rutile waste which was produced by hydrometallurgy process of ilmenite was obtained from Tor Minerals in Lahat, Perak, Malaysia

TiO₂ are the most favored semiconductors due to its superiority photocatalytic performance, effectiveness, cheapness, nontoxicity and good chemical stability [4][5]. Generally, TiO₂ structure can be formed in three phases; rutile, anatase and brookite. The anatase phase are more attracted compare to the rutile and brookite phase due to its suitability as photocatyst, high-temperature stable phase and good band gap with 3.2eV (380nm) while rutile phase had too low band gap with 3.0eV (415nm).

The application potential of TiO₂ photocatyst is varies depends on its band gap, crystallinity, morphology and surface area [6]. The synthesis method are one of the effective strategy to enhance TiO₂ photocatalyst performance due to its affect to their surface area, crystalline phase and particle size [7]. Therefore, the synthesizing method has become the main focus to produce a high-quality of TiO₂ since it's commercially applied.

There are several synthesizing method such as microwave assisted method [8], sol-gel [9], microwave molten salt process [10], solvothermal [11] and caustic hydrothermal treatment [12][13] which were using a different raw material, equipment required and also different experimental step. The microwave assisted method by Suwankar et al., requires a multistep procedure with an expensive microwave oven. The sol-gel method were required an acidic raw material, multistep of procedure and usually producing a bulk TiO₂ either amorphous or poorly crystalline products [14].

Based on our study, the caustic hydrothermal method are the best synthesis method due to their low raw material cost, low equipment cost and also their simple and scalable experimental step. The caustic hydrothermal method are synthesizing the TiO₂ in the powder form and this technique is simply modified [12][15][16]. This method consists of fusion and sulphate process. The fusion process help the raw material to be easily converted into TiO₂ while the sulphate process only for ion exchangeable process [1][16].

Following researchers had reported that acid concentration and treatment time of sulphate process were effecting the growth of TiO₂ [3][17][2][18][19][20][21][22]. However, the acidic waste from sulphate process can create a dangerous to our environmental [23]. Therefore, only a medium acid concentration and short treatment time are introduced in this research work.

The effects of medium acid concentration and short treatment time on the sulphate process were analyzed by EDX to identify the percentage of extracted titanium, FESEM to analyze their growth and XRD to study the crystallinity in our extracted sample.

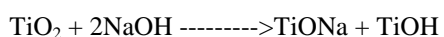
II. MATERIAL AND METHOD

A. Material:

Synthetic rutile waste which were purchased from Tor Minerals in Lahat, Perak, Malaysia, sodium hydroxide (NaOH) sulfuric acid (H₂SO₄) and deionized water.

B. Method:

The fusion process was introduced to converting the synthetic rutile waste into TiONa compound. 10g synthetic rutile waste was fused with 20g of NaOH at 550°C for 3 hours using a high temperature furnace. The product was then washed, filtered and dried at room temperature. The conversion of synthetic rutile waste can be represented as below :



The sulphate process was introduced to converting the TiONa into TiO₂ nanoparticles. The dried TiONa was mixed with three different acid concentrations 1M, 2M and 3M using a 50ml florence flask. These three mixtures were heated simultaneously at 80°C using a digital hot plate with temperature control and stir at 500rpm for 3hours. After the treatment, the white residue obtained then washed with deionized water and ethyl alcohol. The TiO₂ was collected by filtration and dried at 80°C for a 4hours. Lastly, the formed powder was crushed and ground into fine powder using a metal mesh net. After this first batch was done, the same procedure was repeated for the 4hours and 5hours treatment time.

C. Characterization:

The characterization consists of properties and surface morphology characterizations. The properties characterization using the Electron Dispersive (EDX) and X-Ray Diffraction (XRD) while the surface morphology using the Field Emission Scanning Electron Microscope (FESEM).

The EDX analysis was carried out to check the percentage of titanium in synthetic rutile waste and TiO₂ nanoparticles. The distance between sample and the detector is 10cm with 20keV energy resolution. The percentage of titanium (%wt) were measured and tabulated as per Table 1 and Figure 1.

The FESEM analysis was carried out to check the morphology of synthetic rutile waste and the growth of TiO₂ nanoparticles. The FESEM characterization was run at Universiti Teknologi Mara (UiTM) Puncak Alam and the results were shown in Figure 3 and 4 below.

The XRD analysis was carried out to identify the crystallinity phase and particle size of TiO₂ nanoparticles. The characterization was performed using the PANalytical PW3040/60 X'Pert PRO apparatus at the centre of Nanomaterials research Institute of Science, Faculty of Applied Science, Universiti Teknologi Mara (UiTM) Shah Alam. The voltage and anode current used were 40 kV and 30 mA, respectively. The CuK α = 0.15406 nm and the scanning range was from 20° to 90°.

III. RESULT AND DISCUSSION

Figure 1 below shows the elemental composition graph of synthetic rutile waste and TiO₂ nanoparticles in wetweight (wt%) unit which was carried out using the EDX. The EDX spectrum intensity indicates by the ionization energy while the wetweight indicates the counts. Higher the spectrum intensity and counts of each particular element, means the higher the element is presence in that sample. The TiO₂ nanoparticles shown in Figure 1 below were treated with 1M, 2M and 3M acid concentration, 80°C temperature and 4hours sulphate process.

Fig.1(a) shows the synthetic rutile waste with 17eV ionization energy. Besides that, Fig.1(b), 1(c) and 1(d) shows the increasing ionization energy with 41eV, 50eV and 52eV respectively. The shown ionization energy proves that, the TiO₂ nanoparticles has a higher spectrum intensity compared to the synthetic rutile waste. The EDX data in Figure 1 below then was simplified and tabulated as shown in Table 1 below.

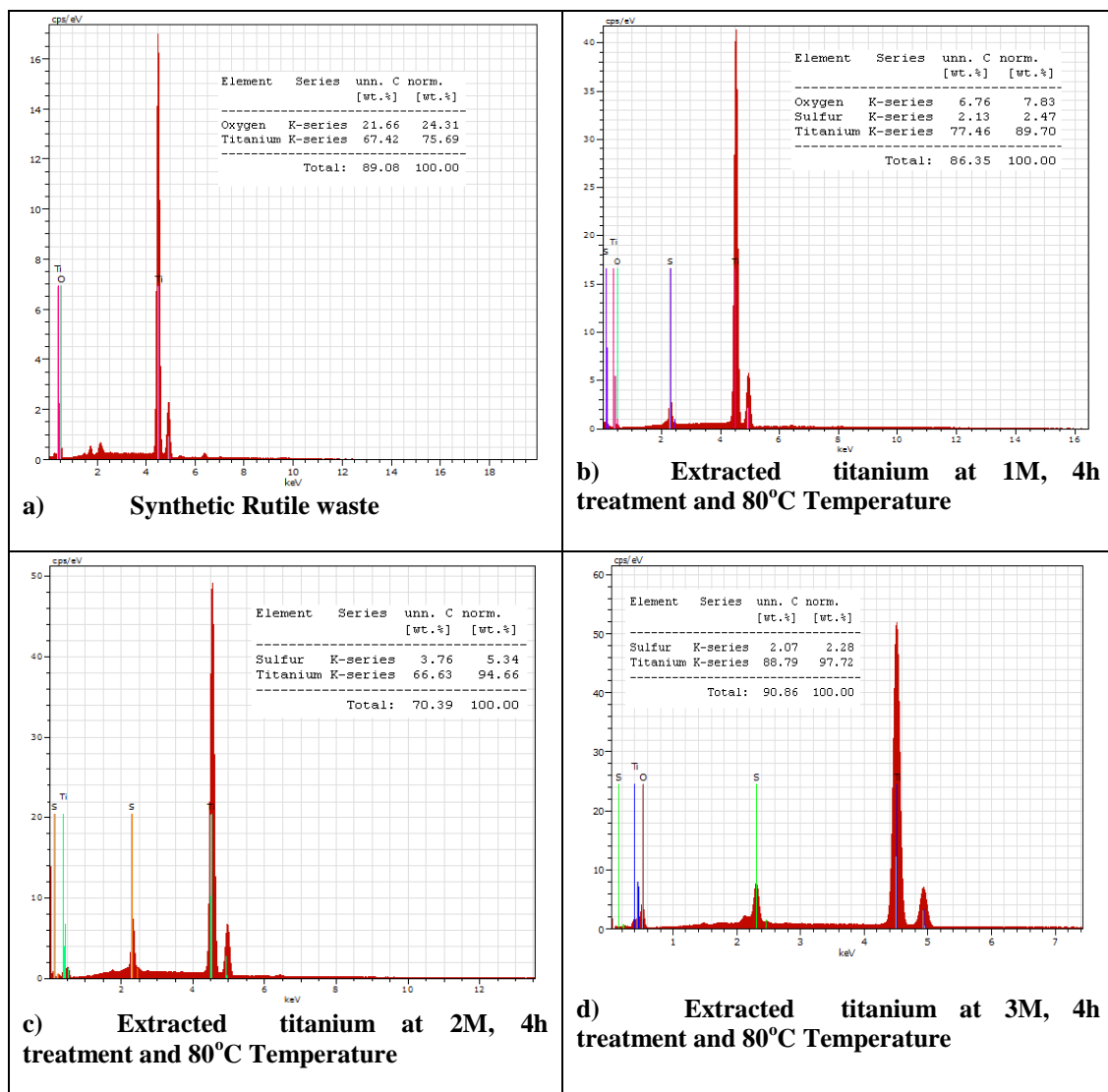


Figure 1 : Elemental composition of (a) Synthetic rutile waste; (b) TiO₂ at 1M; (c) TiO₂ at 2M and (d) TiO₂ at 3M

Based on the tabulated EDX results in Table 1 below, we clearly can see that, the amount of titanium wettage in 1M, 2M and 3M samples were increased by 14%, 19% and 22% respectively compared to the initial titanium wettage in synthetic rutile waste. Therefore, this results prove that the acid concentration of sulphate process can affect the purity of TiO₂ same as reported by previous researchers [2][3][17][21]. The results also shows that the higher the acid molarity, the higher the titanium composition on that sample. Due to E. M. Mahdi, the higher the sulphuric acid molarity, the higher the protons (H⁺) and sulphate ion which lead to the higher leaching rate [15].

Table 1: Elemental composition of synthetic rutile waste and TiO₂ nanoparticles in wettage (wt%).

Elements (in wt %)	
Sample	Ti
Synthetic Rutile	75.69
Extracted titanium at 1M and 4h treatment	89.70
Extracted titanium at 2M and 4h treatment	94.66
Extracted titanium at 3M and 4h treatment	97.72

Figure 2 below shows the graph of extracted titanium wettage (wt%) versus treatment time (3h, 4h and 5h) for three acid concentration (1M, 2M and 3M). For the 1M and 2M acid concentration, the obtained titanium wettage are 85.96%, 88.17%, 93.00% and 92.97%, 94.48%, 95.22% for 3h, 4h and 5h treatment time respectively. For 3M acid concentrations, the obtained titanium wettage also increase 94.90%, 97.81% and 99.85% respectively. From this result, we can conclude that, the longer the leaching time, the higher the titanium wettage can be extracted. The result was similar to that reported by following researchers [2][18][22].

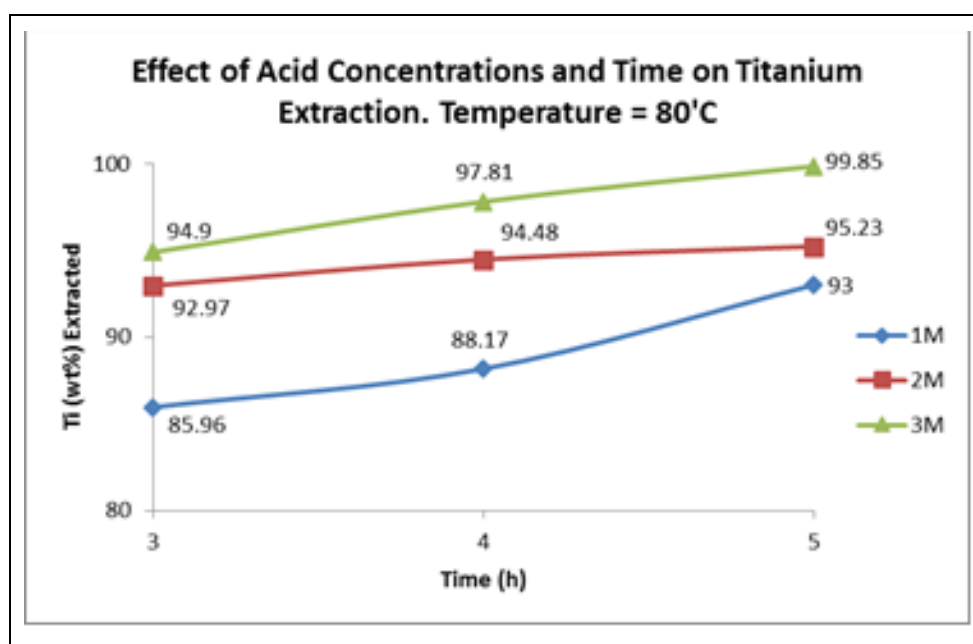


Figure 2: Effect of treatment time on varies acid concentrations at 80°C temperature.

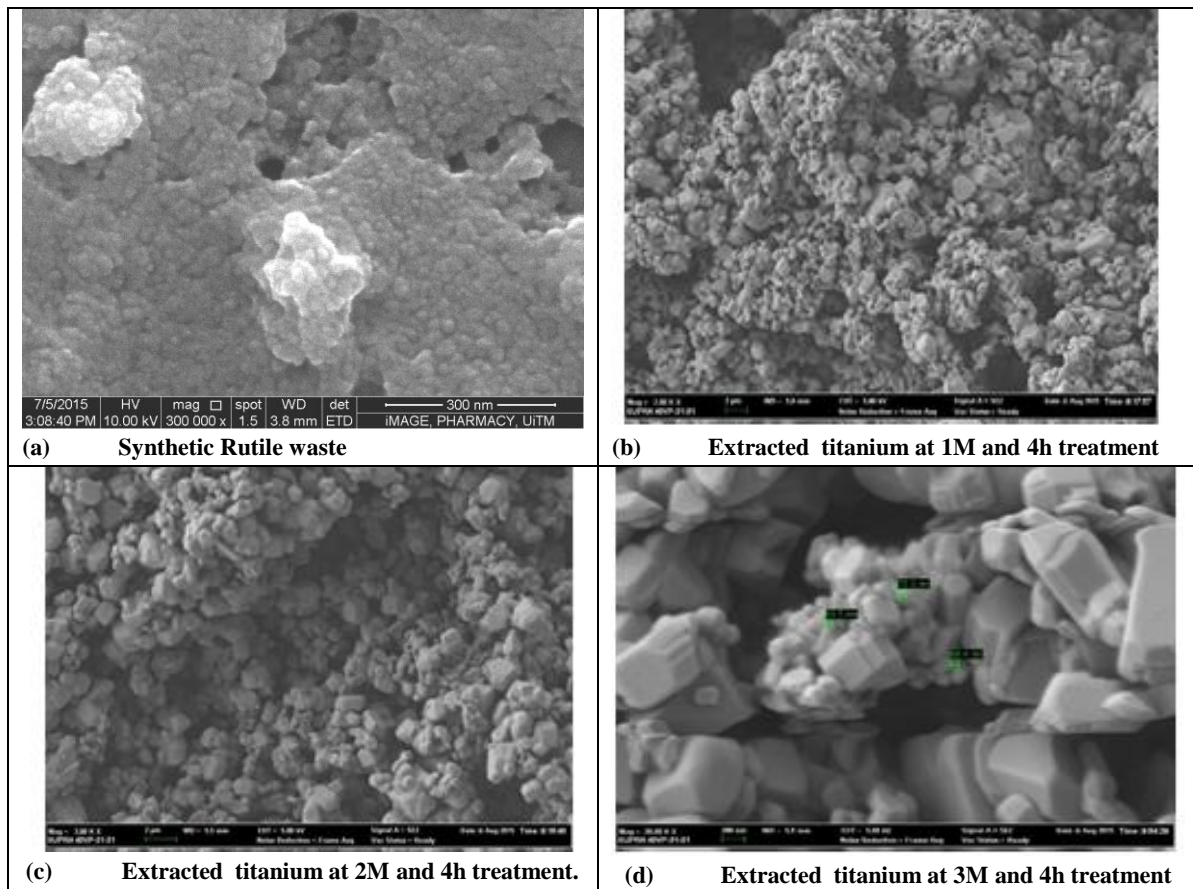


Figure 3: The morphology of 3(a):Synthetic rutile waste; 3(b): 1M TiO₂; 3(c): 2M TiO₂ and Fig 3(d): 3M TiO₂ at 4h treatment time

Figure 3 above shows the morphology of samples which were carried out by FESEM. The sample's morphology are shown in 3(a) synthetic rutile waste; 3(b) 1M TiO₂; 3(c) 2M TiO₂ and 3(d) 3M TiO₂. Based on figure 3 above, we can see the morphology 3(a) are compact and aggregated while the agglomeration states of 3(b), 3(c) and 3(d) are varies and in spherical particles. The 3(b) and 3(c) shows a relatively loose and less agglomeration compared to the 3(a) structure. The 3(d) shows a significant spherical particles which were clearly grown with a large surface area due to the less agglomeration.

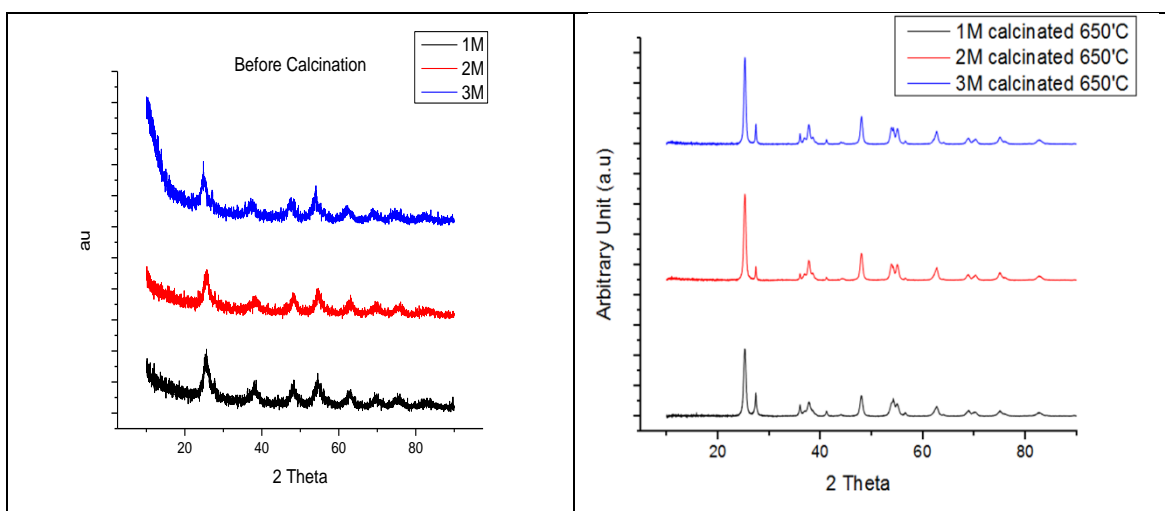


Figure 4: The XRD results of (a) 1M, 2M, and 3M extracted titanium before calcination and (b) 2M treated samples before and after calcination:

Figure 4 above shows the XRD results of 4(a) 1M, 2M and 3M TiO₂ before calcination and 4(b) 1M, 2M and 3M TiO₂ after calcination. The shown XRD peak were matched with the titanium dioxide patterns, ICSD ref no. 03-065-5714 (Anatase) and 01-086-0147 (Rutile). The sharp and strong diffraction peak of 4(b) proves that they has a better crystalline phase and the small diffraction peak indicated that they has a smaller crystallite size compared Figure 4(a).

By using the Scherrer's equation [$D=0.9\lambda/\beta \cos \theta$], we calculate the average crystal size of the TiO₂ particles. The λ is the CuK α radiation ($\lambda = 0.15406$ nm), β is the full width at half maximum (FWHM) intensity of the peak in radians and θ is the Bragg's diffraction angle. Figure 5 below shows the crystallite size of 2M TiO₂ calculated by Scherrer's equation. From this figure, its clearly shows the 2M TiO₂ has a small crystallite size with less than 20nm.

2 θ	θ	cos θ	sin θ	FWHM (°)	FWHM (Radian)	$\beta \cos \theta$	Particle Size (nm)
27.4096	13.7048	0.419021	0.907976	0.5353	0.0175	0.007333	18.9012
36.0564	18.0282	0.681229	-0.73207	0.8029	0.014	0.009537	14.53255
39.2051	19.60255	0.729645	0.683826	0.8029	0.014	0.010215	13.56825
44.1628	22.0814	-0.99593	-0.09013	0.8029	0.014	-0.01394	9.94046
48.0693	24.03465	0.455296	-0.89034	1.0706	0.0187	0.008514	16.27899
54.3324	27.1662	-0.44633	0.894867	0.5353	0.0175	-0.00781	17.7446

Figure 5: The crystallite size of 2M TiO₂ calculated by Scherrer's equation.

IV. CONCLUSION

TiO₂ was successfully synthesized via a caustic hydrothermal decomposition followed by medium conditions of sulphate process. The effect of acid concentration and treatment time of sulphate process were examined and analysed. The EDX, FESEM and XRD results prove that the acid concentration and time were affected the purity, growth and crystallinity of TiO₂. Based on all analysis and discussion made, we conclude that the 2M and 3M TiO₂ results shows a similar and almost the same result. Therefore, for further laboratory works, we choose to investigate the optimum condition of sulphate process within 2M and 3M acid concentration with varies temperature and ratio.

REFERENCES

- [1] K. Thamaphat, P. Limsuwan, and B. Ngotawornchai, "Phase Characterization of TiO₂ Powder by XRD and TEM," *Nat. Sci.*, vol. 42, pp. 357–361, 2008.
- [2] C. Sasikumar, D. S. Rao, S. Srikanth, B. Ravikumar, N. K. Mukhopadhyay, and S. P. Mehrotra, "Effect of mechanical activation on the kinetics of sulfuric acid leaching of beach sand ilmenite from Orissa, India," *Hydrometallurgy*, vol. 75, no. 1–4, pp. 189–204, 2004.
- [3] W. Zhang, Z. Zhu, and C. Y. Cheng, "A literature review of titanium metallurgical processes," *Hydrometallurgy*, vol. 108, no. 3–4, pp. 177–188, 2011.
- [4] J. Shen, M. Shi, B. Yan, H. Ma, N. Li, and M. Ye, "Ionic liquid-assisted one-step hydrothermal synthesis of TiO₂-reduced graphene oxide composites," *Nano Res.*, vol. 4, no. 8, pp. 795–806, 2011.
- [5] W. Fan, Q. Lai, Q. Zhang, and Y. Wang, "Nanocomposites of TiO₂ and Reduced Graphene Oxide as Efficient Photocatalysts for Hydrogen Evolution," pp. 10694–10701, 2011.
- [6] S. Ngamta, N. Boonprakob, N. Wetchakun, K. Ounnunkad, S. Phanichphant, and B. Inceesungvorn, "A facile synthesis of nanocrystalline anatase TiO₂ from TiOSO₄ aqueous solution," *Mater. Lett.*, vol. 105, pp. 76–79, 2013.
- [7] J. Chen, F. Qiu, W. Xu, S. Cao, and H. Zhu, "Recent progress in enhancing photocatalytic efficiency of TiO₂-based materials," *Appl. Catal. A Gen.*, vol. 495, pp. 131–140, 2015.
- [8] M. B. Suwarnkar, R. S. Dhabbe, a. N. Kadam, and K. M. Garadkar, "Enhanced photocatalytic activity of Ag doped TiO₂ nanoparticles synthesized by a microwave assisted method," *Ceram. Int.*, vol. 40, no. 4, pp. 5489–5496, 2014.
- [9] M. K. Seery, R. George, P. Floris, and S. C. Pillai, "Silver doped titanium dioxide nanomaterials for enhanced visible light photocatalysis," *J. Photochem. Photobiol. A Chem.*, vol. 189, no. 2–3, pp. 258–263, 2007.

- [10] Z. Kožáková, M. Mrlík, M. S. Edlačík, V. Pavlínek, and I. Kuřitka, "Preparation of TiO₂ Powder By Microwave-Assisted Molten-Salt Synthesis," pp. 2–7, 2011.
- [11] H. G. Yang, G. Liu, S. Z. Qiao, C. H. Sun, Y. G. Jin, S. C. Smith, J. Zou, H. M. Cheng, G. Qing, and M. Lu, "Solvothermal Synthesis and Photoreactivity of Anatase TiO₂ Nanosheets with Dominant {001} Facets Solvothermal Synthesis and Photoreactivity of Anatase TiO₂ Nanosheets with Dominant {001} Facets," *Synthesis (Stuttg.)*, no. 8, pp. 4078–4083, 2009.
- [12] H. H. Ou and S. L. Lo, "Review of titania nanotubes synthesized via the hydrothermal treatment: Fabrication, modification, and application," *Sep. Purif. Technol.*, vol. 58, no. 1, pp. 179–191, 2007.
- [13] Y. Zhang, T. Qi, and Y. Zhang, "A novel preparation of titanium dioxide from titanium slag," *Hydrometallurgy*, vol. 96, no. 1–2, pp. 52–56, 2009.
- [14] D. P. MacWan, P. N. Dave, and S. Chaturvedi, "A review on nano-TiO₂ sol-gel type syntheses and its applications," *J. Mater. Sci.*, vol. 46, no. 11, pp. 3669–3686, 2011.
- [15] E. M. Mahdi, M. Hamdi, M. S. M. Yusoff, and P. Wilfred, "Characterization of Titania Nanoparticles Synthesized by the Hydrothermal Method with Low Grade Mineral Precursors," *J. Nano Res.*, vol. 21, pp. 71–76, 2012.
- [16] W. Paulus, P. Devi, and M. Mahmoud, "Fabrication Of Titania Nanotubes By A Modified Hydrothermal Method," *J. Sci. ...*, pp. 15–24, 2011.
- [17] L. Jia, B. Liang, L. Lü, S. Yuan, L. Zheng, X. Wang, and C. Li, "Beneficiation of titania by sulfuric acid pressure leaching of Panzhihua ilmenite," *Hydrometallurgy*, vol. 150, pp. 92–98, 2014.
- [18] S. Zhang and M. J. Nicol, "Kinetics of the dissolution of ilmenite in sulfuric acid solutions under reducing conditions," *Hydrometallurgy*, vol. 103, no. 1–4, pp. 196–204, 2010.
- [19] C. Li, B. Liang, and L. H. Guo, "Dissolution of mechanically activated Panzhihua ilmenites in dilute solutions of sulphuric acid," *Hydrometallurgy*, vol. 89, no. 1–2, pp. 1–10, 2007.
- [20] A. Mehdilo and M. Irannajad, "Iron removing from titanium slag for synthetic rutile production," *Physicochem. Probl. Miner. Process.*, vol. 48, no. 2, pp. 425–439, 2012.
- [21] C. Li, B. Liang, H. Song, J. Q. Xu, and X. Q. Wang, "Preparation of porous rutile titania from ilmenite by mechanical activation and subsequent sulfuric acid leaching," *Microporous Mesoporous Mater.*, vol. 115, no. 3, pp. 293–300, 2008.
- [22] S. M. Ali, "Production of Nanosized Synthetic Rutile from Ilmenite Concentrate by Sonochemical HCl and H₂SO₄ Leaching," vol. 33, no. 2, pp. 29–36, 2014.
- [23] E. Law and D. a Lane, "Pollution Caused by Waste From the Titanium Dioxide Industry : Directive 89 / 428," vol. 14, no. 2, 1991.